Electronic Supplementary Material (ESI) for Journal of Materials Chemistry A.

Supporting Information

Intercalation-conversion hybrid mechanism enables covalent organic framework with superior Li-ion storage

Huabin Kong,[†*a] Yaying Guan,[†a] Wenlu Sun,[a] Jun Wang,[a] Lu Chen,[a] Jianxin Ou,[a] Luting Xie,[a] Fang Fu,[a] Hui Zhang,[*b] and Hongwei Chen[*a]

Prof. H. Kong, Y. Guan, W. Sun, J. Wang, L. Chen, J. Ou, L. Xie, Prof. F. Fu, Prof. H. Chen
[a]Department of Materials Science and Engineering, Huaqiao University, Xiamen, 361021, China

Prof. H. Zhang,
[b]National Key Laboratory of High-efficiency Utilization of Coal and Green Chemical Engineering, Ningxia University,Yinchun, 750021, China.

† These authors contributed equally to this work

Corresponding authors:
*Huabin Kong, E-mail: konghuabin@hqu.edu.cn
*Hui Zhang, E-mail:zhang_hui0058@nxu.edu.cn
*Hongwei Chen, E-mail: hwchen@hqu.edu.cn

Material Characterizations

The composition and purity of the material were characterized by X-ray diffraction (XRD) on Bruker D8-advance X-ray diffractometer with Cu-Kα radiation (λ=1.5418 Å), using an operating voltage and current of 40 kV and 40 mAy. FTIR spectrums were collected using a Thermoscientific Nicolet 6700 spectrometer. Raman spectra were recorded using a Jobin Yvon LabRam HR 800 confocal micro-Raman system. SEM images were obtained with a FEI Quanta 400 FEG equipped with EDX (Apollo 40 SDD) operated at 10 kV. TEM images were recorded using a Tecnai G2 F20 S-TWIN at 200 kV. TEM images were recorded using a Tecnai G2 F20 S-TWIN at 200 kV. The BET surface of samples was measured using Quantochrome Autosorb instrument. XPS spectra were collected using Thermo Scientific ESCALAB 250Xi with Al Ka radiation. Combined DTA-TG measurement was conducted in a SETARAM DSC−141 at a heating rate of 10 K min^{-1} in air atmosphere. The absorbance of I_2 solution was measuredby the UV–vis spectrophotometer (PG,TU-1900).

Electrochemical Measurements

The electrochemical evaluation was performed on 2032-type coin cells. The prepared electrode material, carbon black and poly(vinyl difluoride) (PVDF) were mixed in a weight ratio of 7:2:1. Slurry of the mixture was stirred for 12 h and pasted on Ti foil, followed by the electrode film being dried in vacuum at 100 °C for 12 h. The average mass loading of active materials was ∼1.0 mg cm^{-2}. Lithium ion batteries (LIBs) were assembled in an Ar-filled glove box by pairing VCOF@CNT as the cathode electrode with Li metal as the anode electrode, with 1.0 M LiTFSi DOL/DME-based electrolyte.

During the assembly of cells, a layer of carbon paper was placed between the cathode and the membrane to suppress the shuttle effect of iodine ions The cyclic voltammetry (CV) measurement was performed on CHI604C electrochemical workstation with a voltage range from 3.3 to 1.0 V. The galvanostatic charge/discharge measurements were performed on a NEWARE battery testing system. The I-VCOF@CNT electrode was activated for 100 cycles at a aurrent density of 1 C. For the GITT tests, the cell was discharged/charged at 0.1 C with current pulse duration of 15 min and interval time of 30 min.

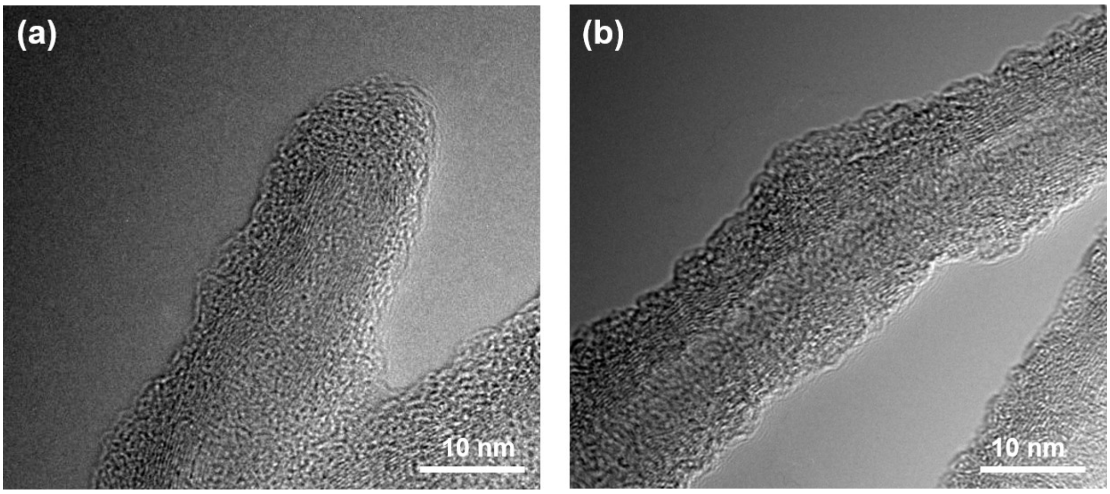

Fig. S1 HRTEM images of I-COF@CNT.

Table S1. The results of Elemental analysis MWCNT, VCOF and I-VCOF@CNT.

Samples	**N wt%**	**C wt%**	**H wt%**
MWCNT	0.05	92.55	0.30
VCOF	13.69	66.91	4.56
I-VCOF@CNT	6.33	73.15	3.01

The content of VCOF and CNT in the I-VCOF@CNT was determined based on the N contents in the MWCNT, VCOF and I-VCOF@CNT as shown in Table S1. The two equations can be described as follows:

$$P_{VCOF} \times N_{VCOF} + P_{CNTs} \times N_{CNTs} = N_{I\text{-}VCOF@CNTs}$$

N_{VCOF}, N_{CNTs} and $N_{I\text{-}VCOF@CNTs}$ correspond to the weight percentages of N and C in VCOF, MWCNTs and the I-VCOF@CNT composite. P_{VCOF} and P_{CNTs} correspond to the mass percentages of VCOF and CNTs in the I-VCOF@CNT composite. According to calculation, P_{VCOF} and P_{CNTs} are 46.0 % and 54.0% in I-VCOF@CNT, respectively. Combined with the **Fig** 2a, it can be calculated that the contents of I_2, VCOF, and CNT in I-VCOF@CNT are 3.63%, 44.33% and 52.04%, respectively.

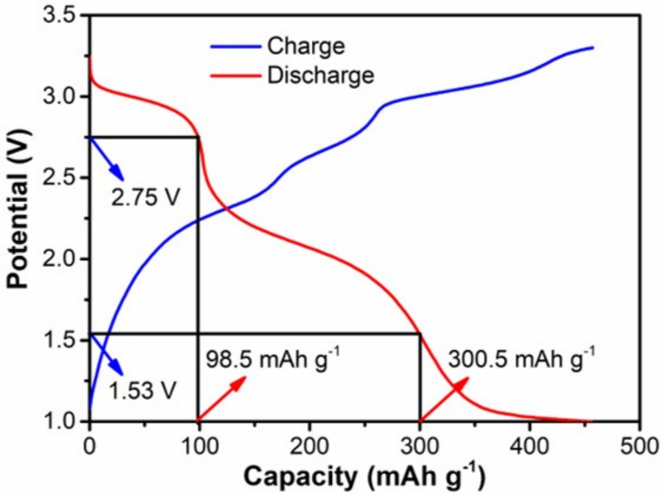

Fig. S2 The 100 th charge/discharge profiles of I-VCOF@CNT at a current density of 1 C.

The discharge capacity of I-VCOF@CNT is 460 mAh g^{-1} at the 100 th cycle. According to the CV curves (Fig. 3a), the capacity in the voltage range of 3.3-2.75 2.75-1.53, and 1.53-1.0 V are provided by the conversion reaction of I_2 and Li^+, the extraction/insertion of Cl^- on the V^{2+}, and the insertion/extraction of Li^+ on the benzene ring, respectively. Therefore, it can be calculated that the conversion reaction of I_2 and Li^+ provides a capacity of 98.5 mAh g^{-1}, the extraction/insertion of Cl^- on the V^{2+} provides a capacity of 202 mAh g^{-1}, and the insertion/extraction of Li^+ on the benzene ring provides a capacity of 159.5 mAh g^{-1}.

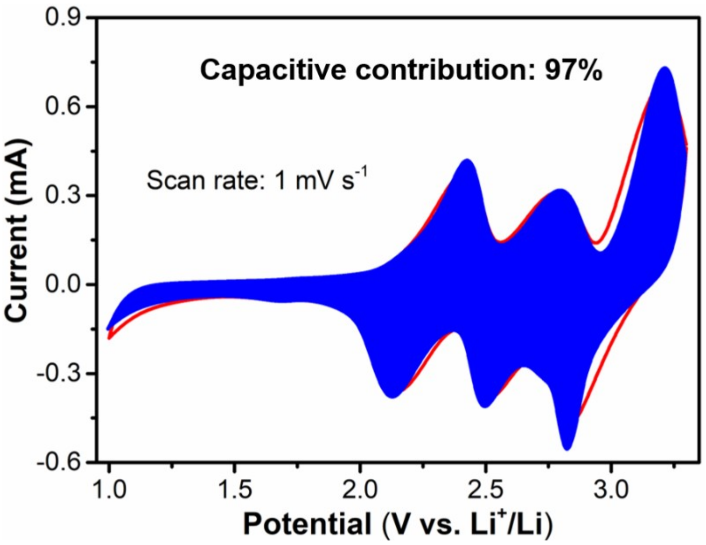

Fig. S3 CV profile of I-VCOF@CNT at 1 mV s^{-1} showing the capacitive contribution (blue region) to the total current.

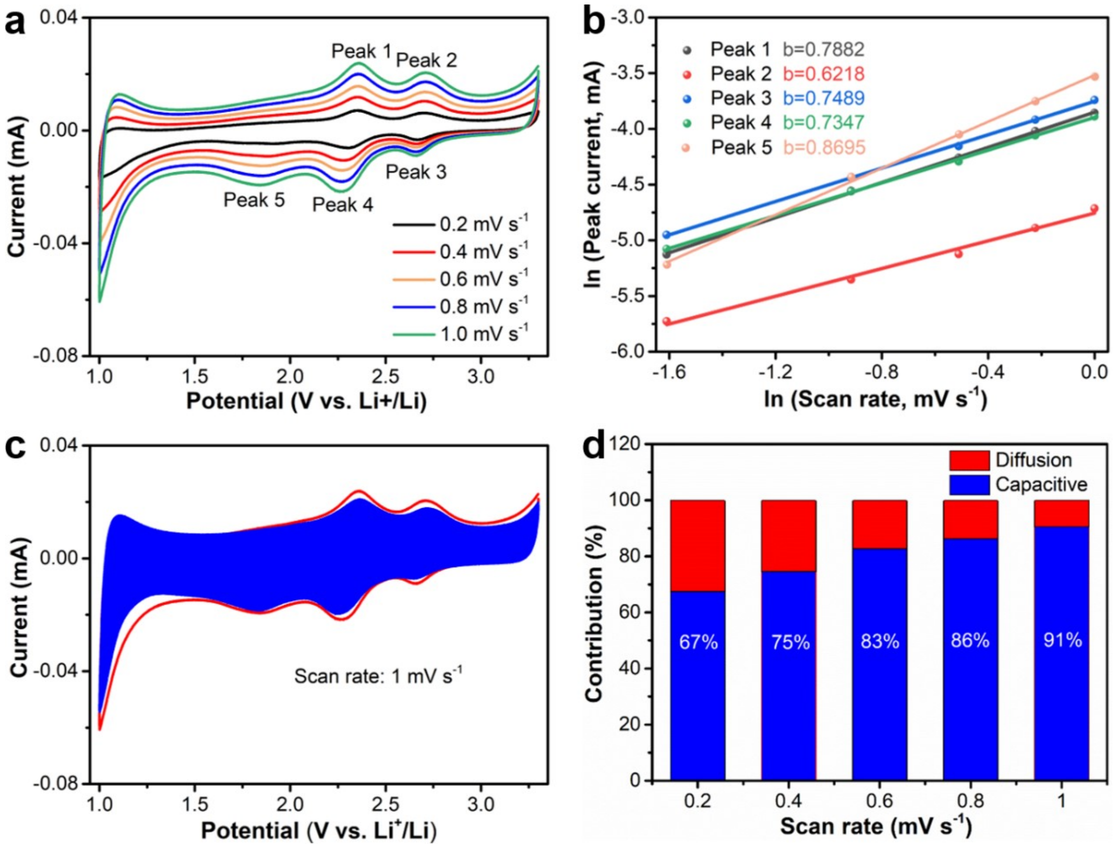

Fig. S4 Kinetics behavior analysis of VCOF@CNT. (a) CV curves at differdent scan rates (b) ln(*i*) versus ln(*v*) plots at specific peak currents (c) CV profile at 1 mV s^{-1} showing the capacitive contribution (blue region) to the total current, (d) The contribution ratio of the capacitive and diffusion controlled at different scan rates.

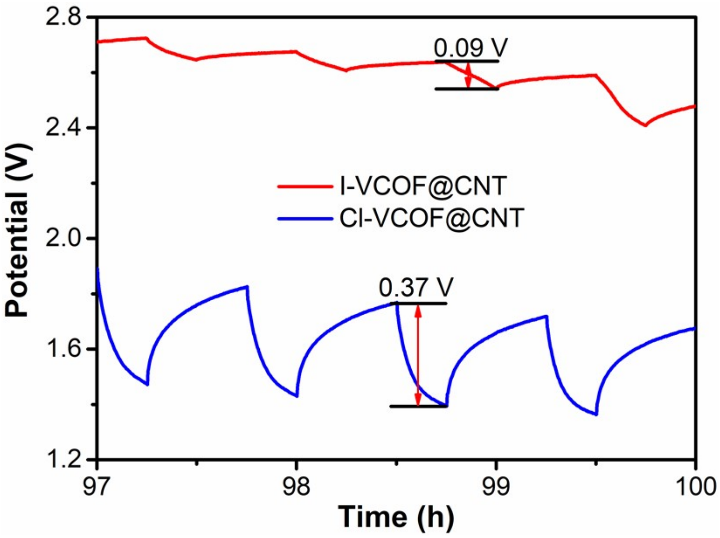

Fig. S5 Potential vs. t curves of the I-VCOF@CNT during discharge process.

The lithium diffusion coefficient was measured by using Galvanostatic intermittent titration technique (GITT) and calculated based on equation as follows.[1,2]

$$D = \frac{4L^2}{\pi\tau}\left(\frac{\Delta E_s}{\Delta E_t}\right)^2$$

Where *L* is lithium ion diffusion length (unit : cm); for compact electrode, it is equal to average thickness of pole piece measured, τ is the relaxation tim e (unit : s), and ΔE_s is the steady-state potential (unit : V) by the current pluse. ΔE_t is the potential change (unit : V) during the constant current pluse after eliminating the iR.

1 G. Fang, G. Fang, Q. Wang, J. Zhou, Y. Lei, Z. Chen, Z. Wang, A. Pan, S. Liang, *ACS Nano*, 2019, 13, 5635-5645.

2 D. T. Ngo, H. T. Le, C. Kim, J-Y Lee, J. G. Fisher, I-D. Kim, C-J. Park, , *Energy Environ. Sci.*, 2015, 8, 3577-3588.

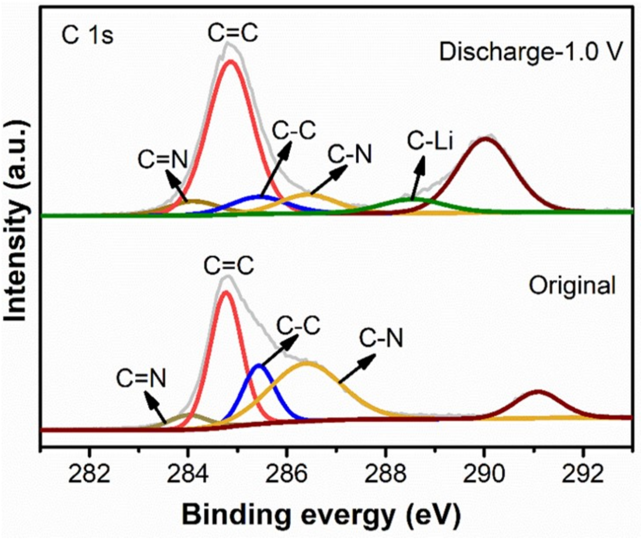

Fig. S6 Ex-situ high-resolution XPS spectra of C 1s region at the original and discharged states.